Available online at www.sciencedirect.com

ScienceDirect

Procedia Structural Integrity 2 (2016) 785–792

Structural Integrity Procedia

www.elsevier.com/locate/procedia

21st European Conference on Fracture, ECF21, 20-24 June 2016, Catania, Italy

Creep-Fatigue Crack Growth Testing and Analysis of Pre-strained 316H Stainless Steel

Ali Mehmanparast[a]*, Catrin M. Davies[b], Kamran Nikbin[b]

[a]*Offshore Renewable Energy Centre, Cranfield University, Cranfield, Bedfordshire MK43 0AL, UK*
[b]*Mechanical Engineering Department, Imperial College London, South Kensington Campus, London SW7 2AZ, UK*

Abstract

Material pre-straining is known to have significant effects of the mechanical response and crack growth behaviour of steels. In this paper, the influence of material pre-straining on the subsequent creep-fatigue crack growth behaviour of Type 316H stainless steel at 550 °C has been examined by performing tests on compact tension specimens that were extracted from blocks uniformly pre-compressed at room temperature. Creep-fatigue crack growth tests on pre-compressed material were performed at the frequency of 0.01 Hz and R-ratio of 0.1. The crack growth data obtained from these experiments have been correlated with the C^* and K fracture mechanics parameters and the results are compared with the existing creep crack growth data on the pre-compressed and as-received material at 550 °C. The results obtained have also been compared with the creep-fatigue data from experiments on weldments where the crack tip was located in the heat affected zone (HAZ). The crack growth behaviour in creep-fatigue tests on pre-compressed material has been found similar to that of HAZ material and are higher than that of the as-received material. Moreover, depending on the loading condition and frequency the crack growth data obtained from creep-fatigue tests on pre-compressed material may be characterized using C^* or ΔK fracture mechanics parameters.

Peer-review under responsibility of the Scientific Committee of ECF21.

Keywords: Cree-Fatigue interaction; Creep; Fatigue; Crack Growth; Stainless Steel

1. Introduction

Material pre-straining is often introduced into high temperature components during fabrication processes. These high temperature components, which can be made of stainless steels such as 316H that is widely used in the UK's

* Corresponding author. Tel.: +44 (0) 1234 758331.
E-mail address: a.mehmanparast@cranfield.ac.uk

Peer-review under responsibility of the Scientific Committee of ECF21.
10.1016/j.prostr.2016.06.101

advanced gas cooled reactors, may be subjected to some degree of cyclic loading, for instance due to start ups and shut downs. Therefore, the crack growth behavior of these components needs to be examined under static and cyclic loading conditions. The influence of material pre-compression on the mechanical response, creep deformation and creep crack growth (CCG) behaviour of Type 316H stainless steel at 550 °C has been previously examined for plastic pre-strain levels ranging from 4% to 12% (Mehmanparast et al., 2013b; Mehmanparast et al., 2016; Mehmanparast et al., 2013a). As shown and explained in Mehmanparast et al. (2013a) the CCG behavior in pre-strained material has been found similar to the trends obtained from 316 weldments, where the crack tip was located in the heat affected zone (HAZ).

In this work, the crack growth behavior of pre-strained 316H stainless steel has been examined under cyclic creep-fatigue loading conditions and the crack growth rates have been correlated with the C^* and K fracture mechanics parameters using the procedures detailed in (Mehmanparast et al., 2011). The loading cycle shape, frequency and R-ratio for the tests performed in this work have been chosen the same as those detailed in (Davies et al., 2009). The cracking behaviour of pre-strained material under cyclic stress loading conditions has also been compared with the experimental data from static load CCG tests on weldment specimens (Davies et al., 2007), pre-compressed (PC) specimens and also the short-term and long-term test data from the as-received (AR) material (Davies et al., 2007; Dean and Gladwin, 2007; Davies et al., 2006b). All tests were performed at 550 °C.

Nomenclature

a	crack length
a_0	Initial crack length
$\dot{a}$	Creep crack growth rate
da/dN	Fatigue crack growth rate per cycle
B	Specimen thickness
B_n	Net-thickness between the side grooves
C	Paris law coefficient
C^*	Steady state creep characterising parameter
D	Constant coefficient in creep crack growth correlation with C^*
D'	Constant coefficient in creep crack growth correlation with K
E	Elastic modulus
f	Frequency
H	Non-dimensional function of specimen geometry and n
K, K_{max}	Stress intensity factor, Stress intensity factor at maximum load
ΔK	Stress intensity factor range
m	Paris law exponent
n	Uniaxial creep power-law stress exponent
N	Cycle number
P	Applied load
R	Load ratio in cyclic tests
t, t_f	Test time, Test duration
W	Specimen width
β	Exponent in correlation of creep crack growth rate with K
ε_f	Tensile strain at failure
$\sigma_{0.2}$	0.2% proof stress
Δ^{LLD}	Load line displacement
$\dot{\Delta}$	Load line displacement rate
$\dot{\Delta}_c$	Creep load line displacement rate
ϕ	Exponent in correlation of creep crack growth rate with C^*
η	Geometry dependent constant
UTS	Ultimate tensile strength

2. Creep-fatigue crack growth test details

2.1. Material pre-straining and specimen manufacture

Four compact tension, C(T), specimens have been used for creep-fatigue tests under cyclic loading conditions. These specimens were extracted from blocks of 316H stainless steel which were uniformly pre-compressed to 8% plastic strain at room temperature. The PC specimens are denoted PC-1, PC-2, PC-3 and PC-4 and their dimensions are summarized in Table 1. The starter crack in all C(T) specimens was introduced using an EDM notch of root diameter 0.25 mm. PC-1, PC-2, PC-3 and PC-4 specimens were side-grooved by 15% on each side. The tensile properties for the AR and PC 316H steel at 550°C are shown in Table 2, where E is the elastic Young's modulus, $\sigma_{0.2}$ is 0.2% proof stress (which is often taken as the yield stress) of the material, UTS is the ultimate tensile strength and ε_f is the tensile strain at failure.

2.2. Loading conditions

The cyclic loading condition was applied using a pneumatic ram. Square shape cycles with 47 s hold time at the maximum load, t_H, and 47 s hold time at the minimum loads, t_L, were applied in the cyclic creep-fatigue crack growth tests. The time for the ram to lower and rise was approximately 4.5 and 1.5 second, respectively. A frequency, f, of 0.01 Hz and load ratio $R = \sigma_{\min}/\sigma_{\max} = 0.1$ was used in all tests. The loading conditions in these tests are reported in Table 1 in terms of $K_{max}(a_0)$ parameter which is the stress intensity factor at the initial crack length a_0, and at the maximum load.

Table 1. Specimen dimensions and loading conditions

Specimen Name	W (mm)	B (mm)	B_n (mm)	a_0 (mm)	$K_{max}(a_0)$ (MPa√m)	t_f (hrs)
PC-1	50	25	17.5	25.0	25.0	194
PC-2	50	25	17.5	25.0	20.0	673
PC-3	50	25	17.5	25.0	22.5	427
PC-4	50	25	17.5	25.0	18.0	503

Table 2. Material properties for the AR and PC 316H steel at 550 °C

Material	E (GPa)	$\sigma_{0.2}$ (MPa)	UTS (MPa)	ε_f (%)
AR	140	177	432	46.70
PC	140	259	441	39.62

3. Analysis of creep-fatigue test data

As shown and discussed in (Mehmanparast et al., 2011) for cyclic crack growth tests at high temperatures, creep is expected to be the dominant cracking mechanism at sufficiently low frequencies of less than approximately 0.01 Hz whereas fatigue is excepted to dominate at high frequencies of greater than approximately 1 Hz. At intermediate frequencies the crack growth is expected to be due to creep-fatigue interaction, therefore the existing procedures for analyzing both static creep and cyclic fatigue crack growth data at elevated temperatures have been considered and briefly described below.

3.1. Creep crack growth

At long times, where a steady state of creep deformation and damage has developed ahead of the crack tip, the CCG rate, $\dot{a}$, may be correlated with the crack tip parameter C^* using a power-law relationship,

$$\dot{a} = DC^{*\phi} \tag{1}$$

where D and ϕ are material constants, which depend on material, temperature and stress state conditions (Webster and Ainsworth, 1994). For CGG tests where the crack tip deformation is dominantly elastic the crack growth may be characterized using the stress intensity factor, K, by a power-law relationship defined as:

$$\dot{a} = D'K^{\beta} \tag{2}$$

where D' and β are material constants.

The C^* fracture mechanics parameter may be determined using the relation (Davies et al., 2006a)

$$C^* = \frac{P\dot{\Delta}}{B_n\left(W - a\right)}H\eta \tag{3}$$

where P is the applied load, $\dot{\Delta}$ is the load line displacement (LLD) rate, B_n is the net thickness between the side-grooves, W is the specimen width, a is the crack length, η is a geometry dependent constant (η = 2.2 for C(T) (Davies et al., 2006a)) and $H = n/(n+1)$ where n is the uniaxial creep power-law stress exponent.

In order to characterize the CCG behavior of a material by the C^* fracture mechanics parameter, the following validity criteria proposed by ASTM E1457 (ASTM, 2007) must be satisfied:

i) The creep crack initiation time must be exceeded, $\Delta a > 0.2$ mm
ii) The transition time, t_T, from an elastic-plastic to a C^* controlled creep crack tip field must be exceeded
iii) The creep load line displacement rate, calculated using the equations given in ASTM E1457 (ASTM, 2007) should constitute at least half of the total load line displacement i.e. $\dot{\Delta}^c/\dot{\Delta}^T \geq 0.5$.

If the last conditions is satisfied the material is conventionally referred to as creep-ductile. When $\dot{\Delta}^c/\dot{\Delta}^T < 0.25$ the material is creep-brittle and the creep crack growth behavior is expected to be characterized by the parameter K.

3.2. Fatigue crack growth

Under predominate fatigue loading conditions, the crack growth rate per cycle, *da/dN*, in the secondary fatigue crack growth region may be characterized using the Paris law (Paris and Erdogan, 1963)

$$\frac{da}{dN} = C\Delta K^{m} \tag{4}$$

where ΔK is the stress intensity factor range, C and m are the power-law coefficient and exponent, respectively, which are strongly dependent on the R ratio and loading frequency.

4. Load line displacement and crack growth behaviour

The load line displacement and crack length data from creep-fatigue tests on PC specimens are plotted against the test time, t, in Figure 1(a) and (b), respectively. As seen in Figure 1(a), the LLD trends for PC specimens are similar, with the highest LLD and shortest test duration corresponding to the test with the highest applied load, PC-1, as expected (see Table 1). It can be seen in Figure 1(b) that apart from Test PC-4, an initiation period is observed for the tests data, where the time for 0.2 mm crack extension is 62, 90 and 180 hrs for test PC-1, PC-2, and PC-3, respectively. In contrast, immediate crack growth is observed in sample PC-4, which has the lowest load applied to the sample, this may be attributed to a reduction in crack tip blunting at lower loads.

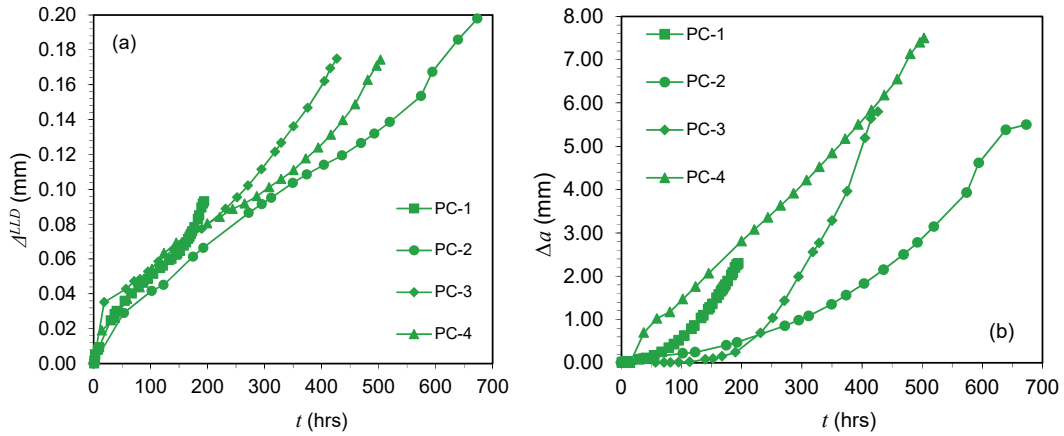

Figure 1. (a) Load line displacement data and (b) crack length data, against test duration for creep-fatigue tests on the PC specimens

5. Crack growth rate data analysis

5.1. Analysis of the C validity criteria*

The *C** validity criteria described in Section 3.3 have been applied on the creep-fatigue test data and the results are shown in Figure 2. In this figure, the valid data points for the PC and HAZ materials have been in solid (green) and hollow (black) symbols, respectively, whereas the invalid data points are shaded in grey. Note that for the creep-fatigue tests the maximum load values have been employed in the analysis. As seen in Figure 2, in all tests expect PC-4 the creep to total LLD rate ratio was above 0.5 for approximately the first half of the test duration, however a fluctuating trend can be observed in PC-4 which remains only a few valid data points from this test. Note that as seen in Table 1, the $K_{max}(a_0)$ applied in this test was the lowest among all creep-fatigue tests performed in this work.

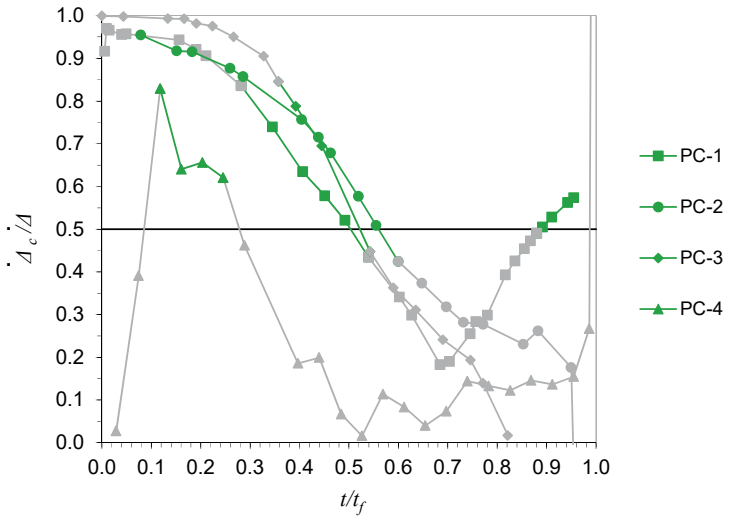

Figure 2. *C** validity criteria for creep-fatigue tests on the PC and HAZ specimens

5.2. Correlation with the C* parameter

The creep crack growth rate from the tests performed on the PC specimens have been correlated with the C^* fracture mechanics parameter and the results are shown in Figure 3 (a). Both valid and invalid data points from creep-fatigue tests are included in this figure. As seen in this figure, although the C^* validity criteria have been applied, the majority of the valid data points appear to be in the 'tail' region and do not have a powetr-law correlation with the C* parameter, except some points at the end of test PC-1. Also seen in this figure is that some of the data points considered invalid from the creep-fatigue tests exhibit a power-law correlation between the CCG rate and the C^* parameter, though except for PC-3, the slopes of these points are much less than that expected from the CCG models (Webster and Ainsworth, 1994) .

The valid CCG rate data obtained from the creep-fatigue tests on the PC material are compared with the static CCG data on the PC, HAZ, short-term AR and long-term AR data in Figure 3 (b). Also included in this figure are the mean fits to these data sets. It can be seen in this figure that the valid data points from creep-fatigue tests on the PC material fall within the experimental data band from the static CCG tests on the PC material. Also seen in this figure is that the valid data from creep-fatigue tests on the PC material fall close to the experimental data band for the HAZ material. Furthermore, this figure shows that for a given value of C^*, the crack growth rate in the creep-fatigue tests on the PC material is around an order of magnitude higher than the short term (i.e. high C^*) AR data and the data follow the long-term (low C^*) trend for the AR material.

It must be noted that the CCG rates and LLD rates employed in C^* calculations are based on the total time and the total LLD rate. It is expected that creep damage and crack growth is a lot more severe at the maximum load, compared to the minimum load, therefore the test time used in $\dot{a}$ and C^* calculations must be 47% of the test time (hold time at the maximum load divided by the cycle period times the number of cycles). This means that the $\dot{a}$ and C^* would shift forward by the same factor which still keeps the CCG trends unchanged.

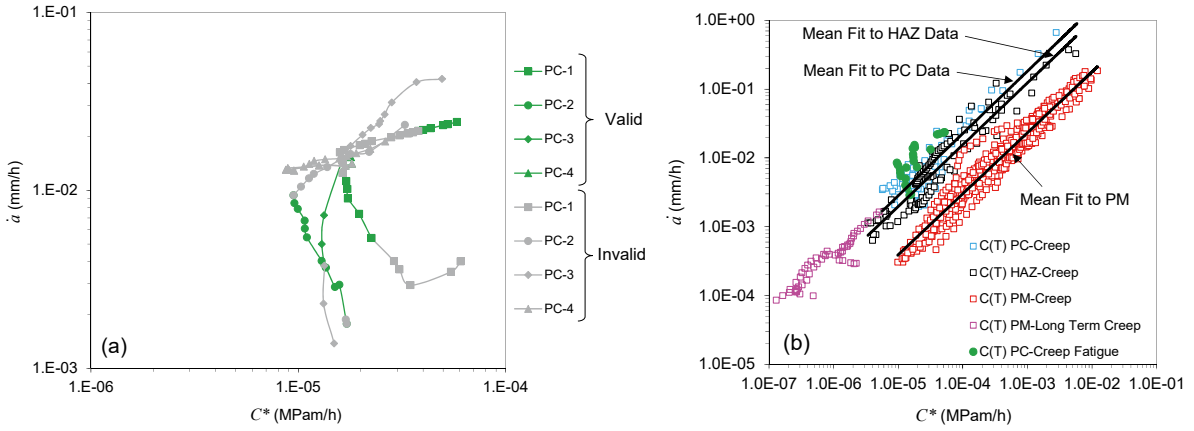

Figure 3. (a) Comparison of the creep-fatigue data from the PC specimens (b) Comparison of the valid creep-fatigue data from the PC specimens with static creep data for the PC, HAZ, short-term AR and long-term AR material

5.3. Correlation with the K_{max} and ΔK parameters

The CCG rate data from the creep-fatigue tests on the PC have been correlated with the stress intensity factor, calculated at the maximum load, and the results are shown in Figure 4. As seen in this figure, the data tend to fall close to each other towards the end of the test, which corresponding to the data points where the creep to total LLD rate ratio is less than below 0.25 (see Figure 2). The crack growth rate per cycle, calculated for the creep-fatigue tests on the PC, have been correlated with the stress intensity factor range and the results are shown in Figure 5. Note that in order to covert CCG rate to the crack growth rate per cycle, the $\dot{a}$ values were divided by 3600 times the frequency which is $f = 0.01$ Hz as recommended in (Mehmanparast et al., 2011). This figure shows that a power-

law trends may be inferred between the crack growth per cycle and ΔK particularly for the latter half of these data sets, which implies that fatigue may dominate the CCG rate behavior

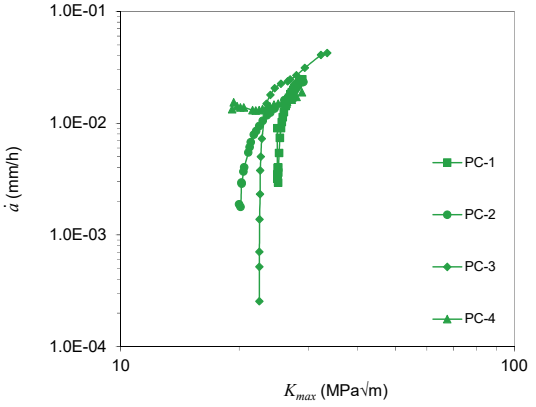

Figure 4. CCG rate correlation with K_{max} for the creep-fatigue tests.

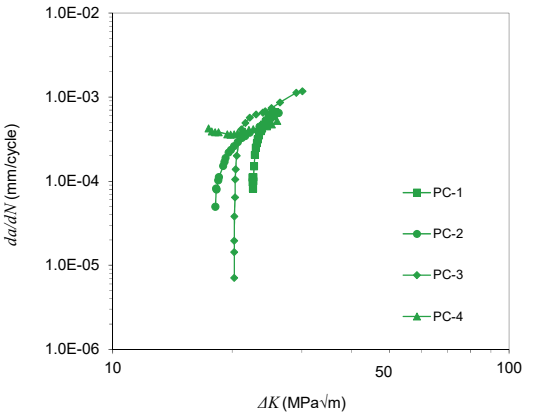

Figure 5. Crack growth rate per cycle correlation with the stress intensity factor range

5. Conclusions

Creep-fatigue interaction tests have been performed on compact tension, C(T), specimens extracted from uniformly pre-compressed blocks of 316H stainless steel. The tests were performed at 550 °C under the R ratio of 0.1 and frequency of 0.01 Hz. The creep crack growth rate correlation with C^* parameter has shown that the valid data points obtained from the cyclic tests on pre-compressed material fall within the experimental data band from the static creep crack growth data on the pre-compressed and HAZ materials. A power-law correlation was found between the fatigue crack growth rate per cycle and the stress intensity factor range for the latter half of the pre-compressed data sets. The experimental data suggest that depending on the frequency, R-ratio and loading conditions one of the failure mechanics may dominate in creep-fatigue tests and the crack growth behavior of the PC 316H steel at 550 °C may be characterized using C^* or ΔK fracture mechanics parameter. Further tests and metallurgical examinations are required to better characterize the creep-fatigue crack growth behavior in 316H at 550 °C.

References

ASTM. (2007) E1457-07: Measurement of Creep Crack Growth Rates in Metals. Annual Book of ASTM Standards. ASTM International, 1012-1035.

Davies CM, Dean DW, Mehmanparast A, et al. (2009) The influence of creep-fatigue interaction on high temperature crack growth in 316 steel weldments. ASME-PVP 26-30 July Prague-Czech republic: proceedings of the International Conference on Pressure Vessels and Piping.

Davies CM, Dean DW, Nikbin KM, et al. (2007) Interpretation of Creep Crack Initiation and Growth Data for Weldments. Engineering fracture mechanics, 74

Davies CM, Kourmpetis M, O'Dowd NP, et al. (2006a) Experimental Evaluation of the J or C* Parameter for a Range of Cracked Geometries. Journal of ASTM International 3: 1-20.

Davies CM, Mueller F, Nikbin KM, et al. (2006b) Analysis of Creep Crack Initiation and Growth in Different Geometries for 316H and Carbon Manganese Steels. Journal of ASTM International 3: 1-20.

Dean DW and Gladwin DN. (2007) Creep Crack Growth Behaviour of Type 316H Steels and Proposed Modifications to Standard Testing and Analysis Methods. International journal of pressure vessels and piping 84: 378-395.

Mehmanparast A, Davies CM, Dean DW, et al. (2013a) Material pre-conditioning effects on the creep behaviour of 316H stainless steel. International journal of pressure vessels and piping 108-109: 88-93.

Mehmanparast A, Davies CM, Dean DW, et al. (2016) Effects of plastic pre-straining level on the creep deformation, crack initiation and growth behaviour of 316H stainless steel. International journal of pressure vessels and piping 141: 1-10.

Mehmanparast A, Davies CM, Dean DW, et al. (2013b) The Influence of Pre-Compression on the Creep Deformation and Failure Behaviour of Type 316H Stainless Steel. Engineering fracture mechanics 110: 52–67.

Mehmanparast A, Davies CM and Nikbin KM. (2011) Evaluation of the Testing and Analysis Methods in ASTM E2760-10 Creep-Fatigue Crack Growth Testing Standard for a Range of Steels. Journal of ASTM International 8: JAI103602-103618.

Paris PC and Erdogan F. (1963) A criticall Analysis of Crack PRopagation Laws. ASME Journal of Basic Engineering 85: 528-534.

Webster GA and Ainsworth RA. (1994) High Temperature Component Life Assessment, London: Chapman and Hall.

Creep-fatigue crack growth testing and analysis of pre-strained 316H stainless steel

Mehmanparast, Ali

2016-07-21

Ali Mehmanparast, Catrin M. Davies, Kamran Nikbin, Creep-Fatigue Crack Growth Testing and Analysis of Pre-strained 316H Stainless Steel, Procedia Structural Integrity, Volume 2, 2016, Pages 785-792

http://dx.doi.org/10.1016/j.prostr.2016.06.101.